AIAA JOURNAL
Vol. 34, No. 5, May 1996

Vibrations and Buckling of Cross-Ply Nonsymmetric Laminated Composite Beams

H. Abramovich,* M. Eisenberger,† and O. Shulepov‡
Technion—Israel Institute of Technology, Haifa 32000, Israel

The exact element method was applied to calculate the natural frequencies, the buckling loads, and the influence of the axial load on the natural frequencies and mode shapes of nonsymmetric laminated composite beams. The theoretical model is using a first-order shear deformation theory and includes the effects of rotary inertia, shear deformation, and coupling between the longitudinal and transverse displacements. A parametric study was performed to investigate the influence of boundary conditions, materials and layup sequence on the buckling loads and natural frequencies of rectangular, cross-ply laminated composite beams.

Introduction

LATERAL vibrations of beams under axial compression have wide applications in the aerospace, civil, and mechanical industries. It is well known that a compressive axial load will tend to decrease all of the bending natural frequencies of a beam, whereas a tensile axial load will increase them. Composite materials are ideal for these structural applications due to their high strength-to-weight and stiffness-to-weight ratios. The classical lamination theory usually used to calculate buckling loads and natural frequencies of laminated composite beams can not accurately predict their behavior, because it neglects the influence of the shear deformation.[1] Therefore, a first-order deformation theory based on the Timoshenko beam theory,[2] that assumes a constant distribution of the shear stress through the thickness of the whole beam is applied to overcome the drawbacks of the classical lamination theory. For cross-ply laminated composite beams the first-order shear deformation theory would yield accurate results such as those predicted by higher order theories.[3] Usually the solution for the buckling loads or for the natural frequencies of a laminated composite beam is obtained either using the finite element approach or the direct method that decouples the equations of motion of the beam. An alternative and very effective approach is the exact element method.[4,5] The exact element method uses the exact shape functions of the beam that are represented by converging infinite series. Using these shape functions, the solution can be obtained with any desired accuracy yielding the exact one. Natural frequencies, buckling loads, and their respective mode shapes can be calculated and plotted, using the dynamic stiffness matrix for any desired set of boundary conditions and assembly of elements. The calculated values of the natural frequencies are those values of frequencies that would cause the dynamic stiffness matrix to become singular. The static behavior, yielding the buckling load, can be calculated by the vanishing of the first natural frequency. The lowest value which would cause the stiffness determinant to vanish would be the buckling load. Very few works in the literature[2] deal with the influence of compressive axial loads on the natural frequencies of laminated composite beams, using adequate theories. One of these studies is a recent work[6] that uses the finite element approach based on a shear deformation theory (Timoshenko beam) to predict the buckling loads and natural frequencies of axially loaded aluminum and graphite-epoxy beams having only two boundary conditions, pinned-pinned and fixed-fixed, and various lengths.

Received Jan. 31, 1995; presented as Paper 95-1459 at the AIAA/ASME/ASCE/AHS/ASC 36th Structures, Structural Dynamics, and Materials Conference, New Orleans, LA, April 10–12, 1995; revision received June 18, 1995; accepted for publication June 20, 1995.

*Senior Lecturer, Faculty of Aerospace Engineering. Member AIAA.
†Associate Professor, Faculty of Civil Engineering. Member AIAA.
‡Graduate Student, Faculty of Aerospace Engineering.

Moreover, the introduction of nonsymmetric laminates would induce a coupling between the axial and lateral motions of the beam causing new significant effects, which are worthwhile to investigate. To the best of our knowledge this topic has not been covered in the literature. Therefore, it is the aim of the present study to use the exact element method, based on a first-order shear deformation theory to predict the stability, the natural frequencies, and their corresponding respective modes and to investigate the interaction occurring in nonsymmetric cross-ply laminated composite beams. The influence of the longitudinal and transverse restraints, materials, and layup sequence on the buckling loads and natural frequencies of rectangular composite beams will be investigated.

Analytical Formulation

The coupled equations of motion for the total lateral deflection w, axial displacement u, and rotation ϕ of the cross section of a rectangular laminated cross-ply composite beam, axially loaded, having constant properties along its length can be shown to be[7,8]

$$A_{11}\frac{\partial^2 u}{\partial x^2} + B_{11}\frac{\partial^2 \phi}{\partial x^2} = I_1\frac{\partial^2 u}{\partial t^2} + I_2\frac{\partial^2 \phi}{\partial t^2} \tag{1}$$

$$A_{55}\left(\frac{\partial \phi}{\partial x} + \frac{\partial^2 w}{\partial x^2}\right) - P\frac{\partial^2 w}{\partial x^2} = I_1\frac{\partial^2 w}{\partial t^2} \tag{2}$$

$$B_{11}\frac{\partial^2 u}{\partial x^2} + D_{11}\frac{\partial^2 \phi}{\partial x^2} - A_{55}\left(\phi + \frac{\partial w}{\partial x}\right) = I_3\frac{\partial^2 \phi}{\partial t^2} + I_2\frac{\partial^2 u}{\partial t^2} \tag{3}$$

where

$$(A_{11}, B_{11}, D_{11}) = c\int_{-h/2}^{h/2} \bar{Q}_{11}(1, z, z^2)\,\mathrm{d}z \tag{4}$$

$$A_{55} = kc\int_{-h/2}^{h/2} \bar{Q}_{55}\,\mathrm{d}z \tag{5}$$

$$(I_1, I_2, I_3) = c\int_{-h/2}^{h/2} \rho(1, z, z^2)\,\mathrm{d}z \tag{6}$$

where h and c are the height and width of the beam, respectively, k is the shear correction coefficient (taken as $\frac{5}{6}$), $\bar{Q}_{11}$ and $\bar{Q}_{55}$ are the stiffness coefficients (see Ref. 7), ρ is the mass density of the beam material, and P is the axial compressive load. The value of $k = \frac{5}{6}$ was chosen in order to compare with available results in the literature, although for better results k should be calculated for each layup.

The following are the boundary conditions associated with the problem:

$$A_{11}\frac{\partial u}{\partial x} + B_{11}\frac{\partial \phi}{\partial x} = P \quad \text{or} \quad u = 0$$
$$A_{55}\left(\phi + \frac{\partial w}{\partial x}\right) - P\frac{\partial w}{\partial x} = 0 \quad \text{or} \quad w = 0 \tag{7}$$
$$B_{11}\frac{\partial u}{\partial x} + D_{11}\frac{\partial \phi}{\partial x} = 0 \quad \text{or} \quad \phi = 0$$

which can be imposed at the beam boundaries $x = 0, L$.

One should note that in the derivations of Eqs. (1–3) it was assumed a priori that the y-direction (perpendicular to the beam axis x) strains vanish, leading to the neglect of the Poisson effect. The consistent four coupled equations of motion of generally layered composite beams as developed by Krishnaswamy et al.[9] and Teboub and Hajela,[10] however, collapse into three coupled equations [Eqs. (1–3)] only for the case of cross-ply laminated beams (see Ref. 9), which is the subject of the present work. Therefore, although Eqs. (1–3) are similar to the equations of motion of a laminated plate undergoing cylindrical bending, they correctly represent the behavior of a cross-ply laminated beam and can be used to predict buckling loads and natural frequencies (see Ref. 9).

Exact Element Method

A detailed review and application of the exact element method can be found in Ref. 4. In what follows, only the essential steps of the method will be highlighted.

For harmonic vibrations, the equations of motion for laminated beams read

$$I_1\omega^2 u + I_2\omega^2\phi + A_{11}\frac{d^2u}{dx^2} + B_{11}\frac{d^2\phi}{dx^2} = 0 \tag{8}$$

$$I_1\omega^2 w + A_{55}\left(\frac{d^2w}{dx^2} + \frac{d\phi}{dx}\right) - P\frac{d^2w}{dx^2} = 0 \tag{9}$$

$$I_2\omega^2 u + I_3\omega^2\phi + D_{11}\frac{d^2\phi}{dx^2} + B_{11}\frac{d^2u}{dx^2} + A_{55}\left(\frac{dw}{dx} + \phi\right) = 0 \tag{10}$$

For symmetrically laminated beams, $B_{11} = I_2 = 0$, and the equations reduce to

$$I_1\omega^2 u + A_{11}\frac{d^2u}{dx^2} = 0 \tag{11}$$

$$I_1\omega^2 w + A_{55}\left(\frac{d^2w}{dx^2} + \frac{d\phi}{dx}\right) - P\frac{d^2w}{dx^2} = 0 \tag{12}$$

$$I_3\omega^2\phi + D_{11}\frac{d^2\phi}{dx^2} + A_{55}\left(\frac{dw}{dx} + \phi\right) = 0 \tag{13}$$

Here we see that the first equation is uncoupled from the other two. These are coupled and are similar to the equations for the Timoshenko beam model that includes the effect of shear deformations and rotary inertia.

If we normalize Eqs. (8–10) using the relation $\xi = x/L$, and choose for the solution the following polynomial series:

$$u = \sum_{i=0}^{\infty} u_i\xi^i \tag{14}$$

$$w = \sum_{i=0}^{\infty} w_i\xi^i \tag{15}$$

$$\phi = \sum_{i=0}^{\infty} f_i\xi^i \tag{16}$$

substitution of these expressions and their derivatives in the differential equations yields

$$I_1L^2\omega^2\sum_{i=0}^{\infty} u_i\xi^i + I_2L^2\omega^2\sum_{i=0}^{\infty} f_i\xi^i + A_{11}\sum_{i=0}^{\infty}(i+1)(i+2)u_{i+2}\xi^i + B_{11}\sum_{i=0}^{\infty}(i+1)(i+2)f_{i+2}\xi^i = 0 \tag{17}$$

$$I_1L^2\omega^2\sum_{i=0}^{\infty} w_i\xi^i + (A_{55} - P)\sum_{i=0}^{\infty}(i+1)(i+2)w_{i+2}\xi^i + A_{55}L\sum_{i=0}^{\infty}(i+1)f_{i+1}\xi^i = 0 \tag{18}$$

$$I_2L^2\omega^2\sum_{i=0}^{\infty} u_i\xi^i + I_3L^2\omega^2\sum_{i=0}^{\infty} f_i\xi^i + B_{11}\sum_{i=0}^{\infty}(i+1)(i+2)u_{i+2}\xi^i + D_{11}\sum_{i=0}^{\infty}(i+1)(i+2)f_{i+2}\xi^i + A_{55}L\sum_{i=0}^{\infty}(i+1)w_{i+1}\xi^i + A_{55}L^2\sum_{i=0}^{\infty} f_i\xi^i = 0 \tag{19}$$

Equating terms with the same power of ξ in these equations, we arrive at the following recurrence formulas for u_{i+2}, w_{i+2}, and f_{i+2}:

$$u_{i+2} = \frac{-1}{(i+1)(i+2)A_{11}}\left[I_1L^2\omega^2u_i + I_2L^2\omega^2f_i - B_{11}L^2(i+1)(i+2)f_{i+2}\right] \tag{20}$$

$$w_{i+2} = \frac{-1}{(i+1)(i+2)(A_{55} - P)}\left[I_1L^2\omega^2w_i + A_{55}L(i+1)f_{i+1}\right] \tag{21}$$

$$f_{i+2} = -\frac{\left[I_3L^2\omega^2f_i + I_2L^2\omega^2u_i - \beta L^2\omega^2(I_1u_i + I_2f_i)\right]}{(i+1)(i+2)D_{11}\left(1 - B_{11}^2/A_{11}D_{11}\right)} + \frac{\left[A_{55}L(i+1)w_{i+1} + A_{55}L^2f_i\right]}{(i+1)(i+2)D_{11}\left(1 - B_{11}^2/A_{11}D_{11}\right)} \tag{22}$$

where

$$\beta = B_{11}/A_{11} \tag{23}$$

and we have all of the u_i, w_i, and f_i coefficients except for the first two that should be found using the boundary conditions. The terms for u_{i+2}, w_{i+2}, and f_{i+2} converge to 0 as $i \to \infty$. For this case we choose as degrees of freedom in the formulation, the axial displacement, the lateral deflection, and the flexural rotation at the two ends of the beam element. At $\xi = 0$ we have

$$u_0 = u(0) \tag{24}$$

$$w_0 = w(0) \tag{25}$$

$$f_0 = f(0) \tag{26}$$

so that the first three terms are readily known from the boundary conditions. The terms u_1, w_1, and f_1 are found as follows. All of the

u_i, w_i, and f_i are linearly dependent on the first two in each series, and we can write

$$u(1) = C_1u_0 + C_2u_1 + C_3w_0 + C_4w_1 + C_5f_0 + C_6f_1 \quad (27)$$

$$w(1) = C_7u_0 + C_8u_1 + C_9w_0 + C_{10}w_1 + C_{11}f_0 + C_{12}f_1 \quad (28)$$

$$f(1) = C_{13}u_0 + C_{14}u_1 + C_{15}w_0 + C_{16}w_1 + C_{17}f_0 + C_{18}f_1 \quad (29)$$

The 18 coefficients C are functions of the axial, shear, and flexural stiffness of the element. C_1, for example, is the value of $u(1)$ when $u_0 = 1$ and $u_1 = w_0 = w_1 = f_0 = f_1 = 0$ calculated from Eqs. (14–16) using the recurrence formulas in Eqs. (20–22). The number of terms that are used is determined for each case according to a preset criteria: it could be until the contribution of the next element in the series is less than an arbitrary small ε (in most of the cases ε was chosen as 10^{-18}) or until the C_i values [Eqs. (27–29)] converge completely (for the accuracy of the computer). For each of the 18 coefficients C_i, the number of terms may be different depending on the parameters of the problem. For the derivation of the stiffness matrix, we have to apply unit displacement or rotation at each of the six degrees of freedom for the element, one at a time and calculate all of the terms in the series for u, w, and ϕ using the recurrence formulas. Then the axial force, shear force, and the bending moment at the two ends of the element ($\xi = 0$ and $\xi = 1$) will be the stiffnesses for the member.

Thus, there are six sets of boundary conditions as follows.

Set 1:

$$u(0) = 1; \qquad w(0) = f(0) = u(1) = w(1) = f(1) = 0$$

Set 2:

$$w(0) = 1; \qquad u(0) = f(0) = u(1) = w(1) = f(1) = 0$$

Set 3:

$$f(0) = 1; \qquad u(0) = w(0) = u(1) = w(1) = f(1) = 0$$

Set 4:

$$u(1) = 1; \qquad u(0) = w(0) = f(0) = w(1) = f(1) = 0$$

Set 5:

$$w(1) = 1; \qquad u(0) = w(0) = f(0) = u(1) = f(1) = 0$$

Set 6:

$$f(1) = 1; \qquad u(0) = w(0) = f(0) = u(1) = w(1) = 0$$

Corresponding to these six sets there are six solutions: U_i; $i = 1, 6$ for $u(\xi)$, W_i; $i = 1, 6$ for $w(\xi)$, and F_i; $i = 1, 6$ for $f(\xi)$ that are found using Eqs. (24–26) and (27–29). These are the dynamic shape functions for the laminated beam model as these are frequency dependent. Then, the holding actions, i.e., stiffnesses, are

$$S(1, i) = -(A_{11}/L)U_{i,1} - (B_{11}/L)F_{i,1} \quad (30)$$

$$S(2, i) = -(A_{55}/L)[W_{i,1} + F_{i,0}] + (P/L)W_{i,1} \quad (31)$$

$$S(3, i) = -\left(D_{11}/L^2\right)F_{i,1} - \left(B_{11}/L^2\right)U_{i,1} \quad (32)$$

$$S(4, i) = \frac{A_{11}}{L}\sum_{k=1}^{\infty} kU_{i,k} + \frac{B_{11}}{L}\sum_{k=1}^{\infty} kF_{i,k} \quad (33)$$

$$S(5, i) = \frac{A_{55}}{L}\left[\sum_{k=1}^{\infty} kW_{i,k} + \sum_{k=1}^{\infty} kF_{i,k}\right] - \frac{P}{L}\sum_{k=1}^{\infty} kW_{i,k} \quad (34)$$

$$S(6, i) = \frac{D_{11}}{L^2}\sum_{k=1}^{\infty} kF_{i,k} + \frac{B_{11}}{L^2}\sum_{k=1}^{\infty} kU_{i,k} \quad (35)$$

The natural frequencies of vibration for the member are the values of ω that cause the dynamic stiffness matrix for the element to become singular. Vanishing of the first natural frequency would yield the buckling load. A simple search routine is applied to find these values up to the desired accuracy.

Numerical Results and Discussion

Based on the formulation of the problem presented in the preceding section, buckling loads, natural frequencies, and their interaction were computed using the exact element method for several boundary conditions, materials, number of layers, and stacking sequences and are presented in the form of tables and figures. Table 1 presents the mechanical properties of the materials used for the present calculations. The influence of the end conditions, both longitudinal (movable or immovable ends) and transverse restraints, as well as the influence of the number of layers and its sequence on the buckling load λ is presented in Table 2 for Kevlar®–epoxy and in Table 3 for glass–epoxy and carbon–epoxy. Table 2 presents also a comparison with the exact results of Ref. 8 yielding very good agreement. Note that the exact results of Ref. 8 are also numerical ones, with a finite accuracy. Therefore, the small deviations can be attributed to the accuracy of Ref. 8. As expected, and this holds true for all of the three materials, for symmetrical layup (0/90/0 deg or 0/90/90/0 deg) the longitudinal displacement u does not influence the buckling parameter λ, with the clamped–clamped boundary

Table 1 Mechanical properties

Material	E_{11}, kg/mm^2	E_{22}, kg/mm^2	G_{12}, kg/mm^2	ν_{12}	Q_{11}, kg/mm^2	Q_{12}, kg/mm^2	Q_{22}, kg/mm^2	Q_{66}, kg/mm^2
Kevlar–epoxy	5530	370	94.8	0.340	5573	126.8	372.9	94.8
Glass–epoxy	5493	1830	880.0	0.250	5609	467.2	1869.0	880.0
Carbon–epoxy	13,020	601	280.7	0.314	13,080	189.6	603.7	280.7

Table 2 Nondimensional buckling loads,[a] $\lambda = PL^2/D_{11}$

No. of layers, deg	P-P pinned–pinned (immovable ends, $u = 0$)		H-H hinged–hinged (movable ends, $u \neq 0$)		C-C clamped–clamped (movable and immovable)		C-P clamped–pinned (immovable ends, $u = 0$)		C-H clamped–hinged (movable ends, $u \neq 0$)		C-F clamped–free (immovable ends, $u = 0$)	
	Present	Ref. 8	Present	Ref. 8	Present	Ref. 8	Present	Ref. 8	Present	Ref. 8	Present	Ref. 8
[0/90]	7.754	7.765	4.205	4.222	16.794	16.859	10.129	10.157	8.597	8.631	1.052	——
[0/90/0]	9.846	9.843	9.846	9.843	39.109	39.214	20.084	20.104	20.084	20.104	2.466	——
$[0/90]_2$	9.551	9.550	8.445	8.444	33.666	33.663	17.688	17.681	17.252	17.250	2.113	——
[0/90/90/0]	9.848	——	9.848	——	39.140	——	20.093	——	20.093	——	2.467	——
$[0/90]_3$	9.731	9.729	9.229	9.228	36.782	36.772	19.048	19.040	18.852	18.847	2.309	——

[a]Kevlar–epoxy, $L/r = 500$, $k = 5/6$, $G_{13} = G_{23} = 108$ kg/mm^2, $c = 1$ mm.

Table 3 Nondimensional buckling loads, $\lambda = PL^2/D_{11}$

No. of layers, deg	P-P		H-H		C-C		C-P		C-H		C-F	
	Glass–epoxy[a]	Carbon–epoxy[b]	Glass–epoxy[a]	Carbon–epoxy[b]	Glass–epoxy[a]	Carbon–epoxy[b]	Glass–epoxy[a]	Carbon–epoxy[b]	Glass–epoxy[a]	Carbon–epoxy[b]	Glass–epoxy[a]	Carbon–epoxy[b]
[0/90]	9.449	7.371	8.016	3.715	32.052	14.842	16.965	9.207	16.397	7.596	2.004	0.929
[0/90/0]	9.867	9.851	9.867	9.851	39.438	39.185	20.179	20.106	20.179	20.106	2.467	2.466
$[0/90]_2$	9.776	9.523	9.405	8.324	37.601	33.211	19.381	17.484	19.236	17.011	2.352	2.082
[0/90/90/0]	9.868	9.852	9.868	9.853	39.440	39.210	20.180	20.113	20.180	20.113	2.468	2.467
$[0/90]_3$	9.828	9.722	9.662	9.177	38.629	36.605	19.827	18.965	19.762	18.752	2.416	2.296

[a] $L/R = 500$, $k = 5/6$, $G_{13} = G_{23} = 1003.2$ kg/mm^2, $c = 1$ mm.
[b] $L/R = 500$, $k = 5/6$, $G_{13} = G_{23} = 319.0$ kg/mm^2, $c = 1$ mm.

Table 4 First three natural frequencies, in hertz, Kevlar–epoxy[a]

No. of layers, deg	Mode no.	P-P	H-H	C-C	C-P	C-H	C-F
[0/90]	1	0.1491	0.1091	0.2471	0.1834	0.1704	0.0389
	2	0.4360	0.4360	0.6799	0.5648	0.5514	0.2434
	3	1.0305	0.9794	1.3297	1.1619	1.1482	0.6807
[0/90/0]	1	0.2246	0.2246	0.5068	0.3502	0.3502	0.0801
	2	0.8953	0.8953	1.3872	1.1288	1.1288	0.5001
	3	2.0025	2.0025	2.6948	2.3376	2.3376	1.3928
$[0/90]_2$	1	0.1645	0.1546	0.3497	0.2440	0.2413	0.0551
	2	0.6174	0.6174	0.9608	0.7826	0.7800	0.3448
	3	1.3953	1.3852	1.8751	1.6240	1.6215	0.9628
[0/90/90/0]	1	0.2149	0.2149	0.4850	0.3350	0.3350	0.0766
	2	0.8567	0.8567	1.3283	1.0801	1.0801	0.4785
	3	1.9172	1.9172	2.5824	2.2390	2.2390	1.3333
$[0/90]_3$	1	0.1660	0.1617	0.3656	0.2534	0.2523	0.0576
	2	0.6454	0.6454	1.0039	0.8163	0.8152	0.3604
	3	1.4519	1.4475	1.9586	1.6952	1.6941	1.0062

[a] $L/r = 500$, $k = 5/6$, $G_{13} = G_{23} = 108$ kg/mm^2, $c = 1$ mm.

Table 5 First three natural frequencies, in hertz, glass–epoxy[a]

No. of layers, deg	Mode no.	P-P	H-H	C-C	C-P	C-H	C-F
[0/90]	1	0.1364	0.1256	0.2847	0.1992	0.1962	0.0448
	2	0.5023	0.5023	0.7842	0.6384	0.6355	0.2804
	3	1.1410	1.1295	1.5364	1.3281	1.3252	0.7847
[0/90/0]	1	0.1686	0.1686	0.3819	0.2633	0.2633	0.0600
	2	0.6739	0.6739	1.0518	0.8526	0.8526	0.3762
	3	1.5152	1.5152	2.0597	1.7772	1.7772	1.0526
$[0/90]_2$	1	0.1387	0.1361	0.3083	0.2132	0.2125	0.0485
	2	0.5440	0.5440	0.8494	0.6890	0.6883	0.3037
	3	1.2261	1.2234	1.6638	1.4359	1.4352	0.8499
[0/90/90/0]	1	0.1634	0.1634	0.3703	0.2552	0.2552	0.0582
	2	0.6534	0.6534	1.0198	0.8266	0.8266	0.3647
	3	1.4691	1.4691	1.9971	1.7231	1.7231	1.0205
$[0/90]_3$	1	0.1391	0.1379	0.3125	0.2157	0.2154	0.0491
	2	0.5514	0.5514	0.8609	0.6980	0.6977	0.3078
	3	1.2412	1.2400	1.6863	1.4550	1.4547	0.8614

[a] $L/R = 500$, $k = 5/6$, $G_{13} = G_{23} = 1003.2$ kg/mm^2, $c = 1$ mm.

conditions yielding the highest value followed by clamped–hinged (or clamped–pinned), hinged–hinged (or pinned–pinned) and clamped free.

The constraint of the longitudinal movement u has a major influence on the buckling parameter for nonsymmetric layup. Simply supported boundary conditions with immovable ends [pinned–pinned (P-P) in Tables 2 and 3] yield higher buckling loads as compared to movable ends [hinged–hinged, (H-H)], with the difference being the highest for the 0/90 deg configuration. Increasing the number of layers would yield only a minor difference. One should note that the total height of the beam, h, was kept constant while varying the number of layers for all of the comparisons presented throughout the paper. For the clamped–clamped ends [(C-C) in Tables 2 and 3] the nondimensional buckling load λ is not influenced by the longitudinal restraint. A mixed boundary condition, like clamped–pinned [(C-P) in Tables 2 and 3] having immovable longitudinal ends would yield higher buckling loads than the clamped–hinged [(C-H) in Tables 2 and 3] boundary conditions (movable longitudinal ends). The glass–epoxy material seems to be the less sensitive to in-plane boundary conditions, whereas the other two materials, Kevlar- and carbon–epoxy exhibit noticeable differences for restraining the axial movement.

Increasing the number of layers, while keeping the total height of the beam h and the layup sequence constant, would increase the value of λ, with only a slight change for glass–epoxy with P-P or H-H boundary conditions (Table 3) as compared to Kevlar–epoxy and carbon–epoxy (Tables 2 and 3). Comparing symmetrical layup (0/90/90/0 deg) with a nonsymmetric one ($[0/90]_2$ deg) for beams having the same geometrical dimensions shows a clear advantage for the symmetric configuration (for buckling loads), for all of the boundary conditions considered in the present study.

A similar parametric study was performed for the natural frequencies of laminated composite beams. The first three natural frequencies, calculated according to the exact element method, are presented in Tables 4–6 for Kevlar–epoxy, glass–epoxy, and carbon–epoxy, respectively. No comparison was made with other references

Table 6 First three natural frequencies, in hertz, carbon–epoxy[a]

No. of layers, deg	Mode no.	P-P	H-H	C-C	C-P	C-H	C-F
[0/90]	1	0.2094	0.1474	0.3338	0.2510	0.2302	0.0525
	2	0.5891	0.5891	0.9191	0.7669	0.7452	0.3289
	3	1.4062	1.3238	1.7987	1.5750	1.5525	0.9199
[0/90/0]	1	0.3259	0.3259	0.7361	0.5083	0.5083	0.1162
	2	1.3000	1.3000	2.0177	1.6404	1.6404	0.7261
	3	2.9112	2.9112	3.9267	3.4020	3.4020	2.0243
$[0/90]_2$	1	0.2360	0.2206	0.4993	0.3486	0.3444	0.0786
	2	0.8813	0.8813	1.3726	1.1179	1.1138	0.4920
	3	1.9944	1.9784	2.6815	2.3213	2.3173	1.3749
[0/90/90/0]	1	0.3115	0.3115	0.7036	0.4858	0.4858	0.1110
	2	1.2426	1.2426	1.9296	1.5684	1.5684	0.6940
	3	2.7838	2.7838	3.7577	3.2543	3.2543	1.9355
$[0/90]_3$	1	0.2384	0.2317	0.5241	0.3634	0.3616	0.0826
	2	0.9252	0.9252	1.4406	1.1709	1.1692	0.5166
	3	2.0835	2.0766	2.8135	2.4336	2.4319	1.4433

[a] $L/R = 500$, $k = 5/6$, $G_{13} = G_{23} = 319.0$ kg/mm^2, $c = 1$ mm.

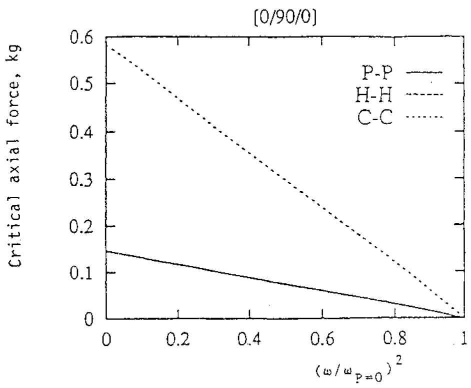

Fig. 1a Variation of the first natural frequency with the axial compression load, symmetric layup [0/90/0 deg].

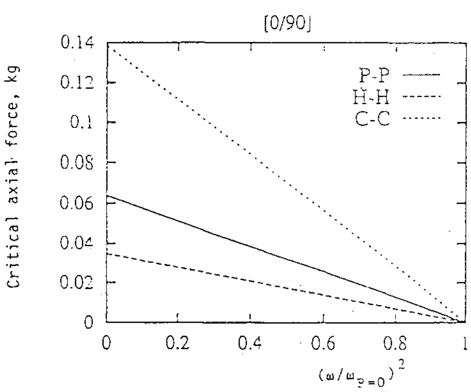

Fig. 1b Variation of the first natural frequency with the axial compression load, nonsymmetric layup [0/90 deg].

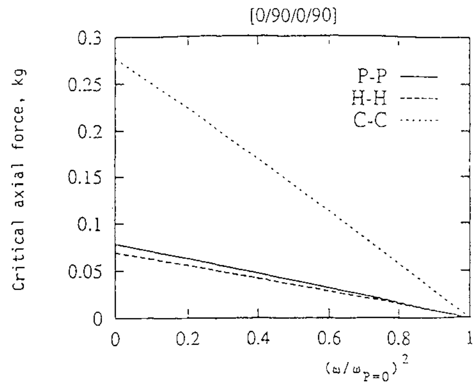

Fig. 1c Variation of the first natural frequency with the axial compression load, nonsymmetric layup $[0/90\ \text{deg}]_2$.

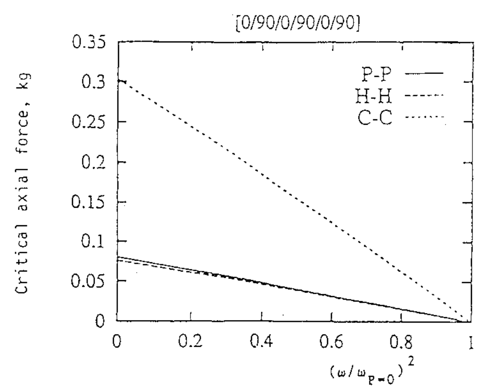

Fig. 1d Variation of the first natural frequency with the axial compression load, nonsymmetric layup $[0/90\ \text{deg}]_3$.

as the exact element method was proved to yield exact results (see Refs. 4 and 5). The conclusions drawn for the buckling behavior hold true also for the natural frequencies of laminated composite beams and are summarized as follows.

1) There is no influence of the in-plane boundary conditions for symmetric layup, but for nonsymmetric ones, restraining the longitudinal movement would increase the natural frequencies of the beam.

2) Increasing the number of layers, while keeping the height of the beam constant, would increase the natural frequencies, both for symmetric and nonsymmetric layups.

3) Comparing symmetric with a nonsymmetric layup for a given beam height and boundary conditions (0/90/90/0 deg vs $[0/90]_2$ deg) shows a greater stiffness for the symmetric configuration, yielding higher natural frequencies.

4) Finally, stiffening the boundary conditions would increase the values of the natural frequencies.

Comparison of the three materials shows that the natural frequencies of carbon–epoxy are the highest, followed by those of glass–epoxy and Kevlar–epoxy (and vice-versa) (see Tables 4–6). Note that the second frequency (mode 2) (Tables 4–6) of a nonsymmetric laminated beam with nominal simply supported boundary conditions is not influenced by the axial restraint, yielding equal values for both pinned–pinned and hinged–hinged boundaries. This is due to the antisymmetric nature of the second mode that causes the superimposed axial mode to vanish.

Next, due to the similar behavior of the buckling loads and the first natural frequencies, interaction curves, buckling load vs the square of the first natural frequency, were calculated (see Figs. 1a–1d, 2a and 2b, and 3a and 3b) and some typical examples are presented.

Figures 1a–1d present the variation of first natural frequency squared with the axial compression load (Kevlar–epoxy) for various layups and boundary conditions. As already stated, the strongest

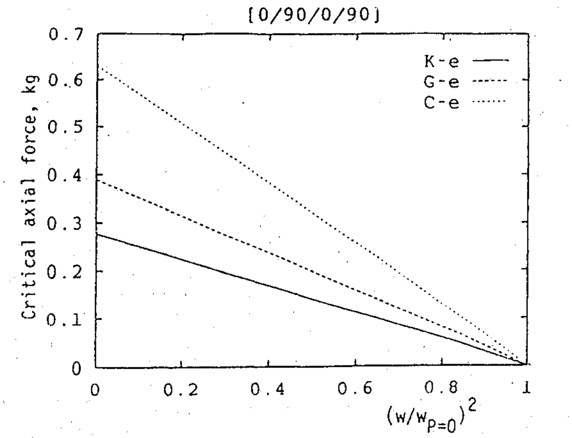

Fig. 2a Variation of the first natural frequency with the axial compression load, clamped–clamped boundary conditions, nonsymmetric layup [0/90 deg]₂: K-e = Kevlar–epoxy, G-e = glass–epoxy, C-e = carbon–epoxy.

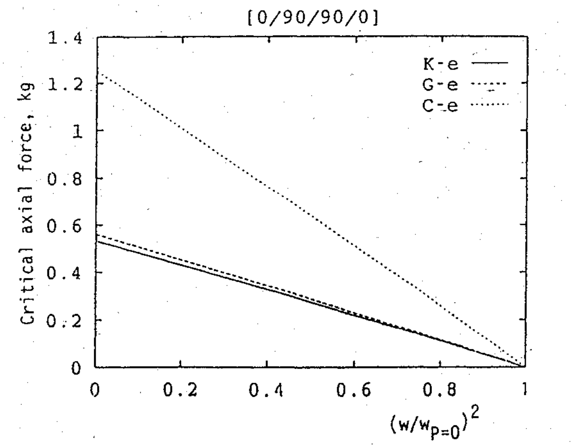

Fig. 2b Variation of the first natural frequency with the axial compression load, clamped–clamped boundary conditions, symmetric layup [0/90/90/0 deg]: K-e = Kevlar–epoxy, G-e = glass–epoxy, C-e = carbon–epoxy.

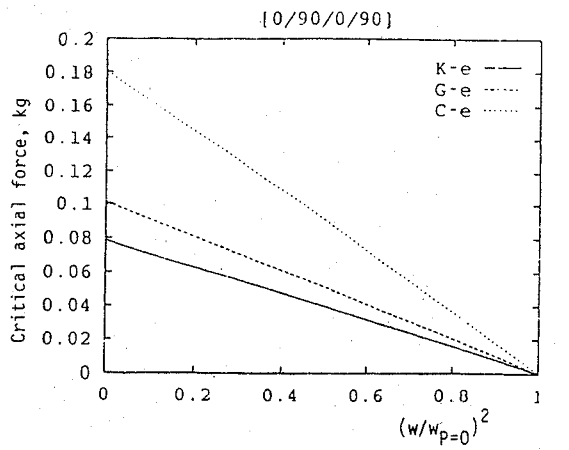

Fig. 3a Variation of the first natural frequency with the axial compression load, pinned–pinned boundary conditions, nonsymmetric layup [0/90 deg]₂: K-e = Kevlar–epoxy, G-e = glass–epoxy, C-e = carbon–epoxy.

influence of the in-plane boundary conditions is for the (0/90 deg) configuration (Fig. 1a).

Figures 2a and 2b present the variation of the first natural frequency squared with the axial compression for clamped–clamped boundary conditions, whereas Figs. 3a and 3b present the same for pinned–pinned boundary conditions for various layups and materials. Note that the inclinations of Kevlar–epoxy and glass–epoxy

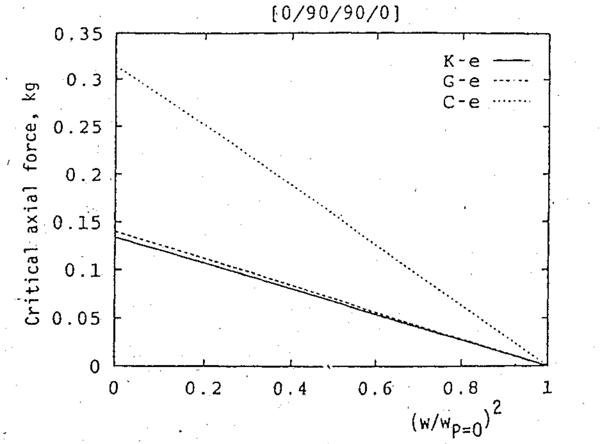

Fig. 3b Variation of the first natural frequency with the axial compression load, pinned–pinned boundary conditions, symmetric layup [0/90/90/0 deg]: K-e = Kevlar–epoxy, G-e = glass–epoxy, C-e = carbon–epoxy.

curves are almost the same for a symmetric layup with a noticeable change for a nonsymmetric one. This is true for both kinds of boundary conditions.

Conclusions

The buckling behavior and natural frequencies of cross-ply composite laminates having nonsymmetric and symmetric layups have been studied using a first-order shear deformation theory. The exact element method was successfully applied to calculate buckling loads and natural frequencies. A parametric study was performed to investigate the influence of boundary conditions, materials, number of layers, and layup sequences on the buckling loads, natural frequencies, and the influence of axial compression loads on the natural frequencies of rectangular, cross-ply laminated composite beams.

References

[1]Abramovich, H., "Shear Deformation and Rotary Inertia Effects of Vibrating Composite Beams," *Composite Structures*, Vol. 20, No. 3, 1992, pp. 165–173.

[2]Abramovich, H., "Natural Frequencies of Timoshenko Beams Under Compressive Loads," *Journal of Sound and Vibration*, Vol. 157, No. 1, 1992, pp. 183–189.

[3]Singh, M. P., and Abdelnasser, A. S., "Random Response of Symmetric Cross-Ply Laminated Composite Beams with Arbitrary Boundary Conditions," *AIAA Journal*, Vol. 30, No. 4, 1992, pp. 1081–1088.

[4]Shulepov, O., "Vibrations of Laminated Beams Using the Dynamic Stiffness Method," M.Sc. Thesis, Faculty of Aerospace Engineering, Technion—Israel Inst. of Technology, Haifa, Israel, Oct. 1993.

[5]Eisenberger, M., "Derivation of Shape Functions for an Exact 4-D.O.F. Timoshenko Beam Element," *Communications in Numerical Methods in Engineering*, Vol. 10, No. 9, 1994, pp. 673–681.

[6]Kosmatka, J. B., "Stability and Natural Frequencies of Axial-Loaded Shear-Deformable Beams Using an Improved Two-Node Finite Element," *Proceedings of the AIAA/ASME/ASCE/AHS/ASC Structures, Structural Dynamics, and Materials Conference* (Hilton Head, SC), AIAA, Washington, DC, 1994, pp. 193–201 (AIAA Paper 94-1331).

[7]Abramovich, H., and Livshits, A., "Free Vibrations of Non-Symmetric Cross-Ply Laminated Composite Beams," *Journal of Sound and Vibration*, Vol. 176, No. 5, 1994, pp. 597–612.

[8]Abramovich, H., "Thermal Buckling of Cross-Ply Composite Laminates Using a First-Order Shear Deformation Theory," *Composite Structures*, Vol. 28, No. 2, 1994, pp. 201–213.

[9]Krishnaswamy, S., Chandrashekhara, K., and Wu, W. Z. B., "Analytical Solutions to Vibration of Generally Layered Composite Beams," *Journal of Sound and Vibration*, Vol. 159, No. 1, 1992, pp. 85–99.

[10]Teboub, Y., and Hajela, P., "Free Vibration of Generally Layered Composite Beams Using Symbolic Computations," *Proceedings of the AIAA/ASME/ASCE/AHS/ASC 35th Structures, Structural Dynamics, and Materials Conference* (Hilton Head, SC), AIAA, Washington, DC, 1994, pp. 182–192 (AIAA Paper 94-1330).